ACCSCIENCE PUBLISHING

Eurasian Journal of Medicine and Oncology

ORIGINAL RESEARCH ARTICLE

# Lactylation-driven diagnostic model for pulmonary hypertension

**Tao Yi[1†], Cuiwen Deng[2†], Junsheng Sun[2], and Qian Lei[2*]**

[1]Department of Emergency Medicine, Longgang Central Hospital of Shenzhen, Shenzhen, China
[2]Department of General Practice, Longgang Central Hospital of Shenzhen, Shenzhen, China

## Abstract

**Introduction:** Pulmonary hypertension (PH) presents a significant global public health challenge, underscoring the need for novel biomarkers and therapeutic strategies.
**Objective:** This study proposes a lactylation-related diagnostic model for PH, aiming to identify potential therapeutic targets.
**Methods:** The GSE15197 dataset was analyzed to identify differentially expressed genes (DEGs). Functional enrichment analyses, including Gene Ontology, Kyoto Encyclopedia of Genes and Genomes, and gene set enrichment analysis (GSEA), were conducted to explore underlying mechanisms. Weighted gene co-expression network analyses (WGCNA) identified two key gene modules. The intersection of significant WGCNA modules, DEGs, and lactylation-associated genes yielded candidate genes related to lactylation in PH. Machine learning methods, particularly random forest and support vector machine, were employed to identify hub genes, ultimately selecting aryl hydrocarbon receptor (AHR), polyribonucleotide nucleotidyltransferase 1 (PNPT1), and RAS p21 protein activator 1 (RASA1). These were incorporated into a diagnostic nomogram, evaluated through receiver operating characteristic curve and decision curve analyses. Immune cell infiltration was assessed using CIBERSORT and single-sample GSEA, while Enrichr was utilized to identify transcription factors and potential therapeutic agents. Molecular docking was performed to assess drug–gene binding affinities.
**Results:** A total of 1,504 genes were upregulated and 1,931 downregulated. Functional enrichment analyses revealed clustering of DEGs in pathways associated with cellular transport, protein degradation, DNA repair, and signal transduction. WGCNA identified two critical modules comprising 1,178 genes, from which 33 candidate genes were derived. Machine learning refined this list to three hub genes (AHR, PNPT1, and RASA1), which formed the basis of a novel lactylation-related diagnostic nomogram validated in an external cohort. Immune dysregulation was evident, and friend leukemia integration 1 was recognized as a key TF. Ten potential drugs demonstrated promising binding affinity to the hub genes.
**Conclusion:** This work introduces a lactylation-based diagnostic model for PH with strong diagnostic potential, though further clinical validation is required.

***Keywords:*** Pulmonary hypertension; Lactylation; Diagnostic value; Molecular docking; Immune cell infiltration

[†]*These authors contributed equally to this work.*

***Corresponding author:**
Qian Lei
(leiqian-hunan@whu.edu.cn)

**Citation:** Yi T, Deng C, Sun J, Lei Q. Lactylation-driven diagnostic model for pulmonary hypertension. *Eurasian J Med Oncol.* 2026;10(2):025190172. doi: 10.36922/EJMO025190172

**Received:** May 6, 2025

**Revised:** June 16, 2025

**Accepted:** July 4, 2025

**Published online:** August 1, 2025

## 1. Introduction

Pulmonary hypertension (PH) is a progressive pulmonary vascular disorder marked by elevated pressure in the pulmonary arteries. A sustained increase in pulmonary artery pressure can eventually result in right heart failure and possibly death.[1]. Clinically, PH is defined by a mean pulmonary arterial pressure >25 mmHg at rest, a pulmonary vascular resistance of 3 Wood units, and a pulmonary capillary wedge pressure of 15 mmHg or lower.[2] At present, the gold standard for diagnosing PH is right heart catheterization;[3] nonetheless, this invasive method lacks a reliable non-invasive alternative for definitive confirmation. Transthoracic echocardiography, although widely used as an initial non-invasive screening tool, primarily serves to guide further diagnostic evaluation rather than confirm diagnosis.[4] Despite these advancements, there remains a critical need for non-invasive diagnostic tools that not only confirm PH but also offer deeper insights into its underlying pathophysiology. Although treatment options for PH have improved, the prognosis remains poor, with a median survival time of approximately 5 years.[5] Moreover, the role of lactylation in PH is not well understood. To address this gap, we developed a lactylation signature model aimed at enhancing diagnostic precision, thereby supporting clinical decision-making.

Lactate, previously viewed as a metabolic byproduct, is now emerging as a pivotal regulator of cellular processes through lactylation – a recently discovered post-translational modification.[6] This modification responds directly to cellular lactate levels and metabolic changes associated with disease, making it a promising candidate biomarker in PH. Zhang *et al.*[7] provided foundational evidence that lactylation of histone lysine residues enhances gene transcription and modulates cellular function. In PH, lactate-driven histone lactylation in lung myofibroblasts promotes profibrotic macrophage activity.[8] Furthermore, mitochondrial reactive oxygen species-mediated glycolytic shifts contribute to histone lactylation and are implicated in hypoxia-induced PH pathogenesis.[9] Emerging evidence also links histone lactylation, N6-methyladenosine modification, and immune homeostasis with PH.[10] Beyond histones, lactylation significantly impacts non-histone protein function, as demonstrated by Wan *et al.*'s[11] research utilizing sophisticated tandem mass spectrometry techniques. Lactate is now recognized not only as a crucial carbon source in cellular metabolism but also as a vital signaling molecule in various physiological phenomena, including chronic inflammation and tumorigenesis.[12,13] In PH, lactate dehydrogenase A (LDHA) plays a key role by promoting lactate production, thereby initiating pulmonary vascular remodeling through the protein kinase B signaling pathway.[14] LDHA-derived lactate also contributes to smooth muscle remodeling and PH progression by lactylating target proteins such as topoisomerase 1 and elastin microfibril interface located protein 1.[15] Given lactylation's dynamic nature, its involvement in PH-specific mechanisms (inflammation, fibrosis, and vascular remodeling), and its detectability across a wide range of protein targets, it holds significant promise as a biomarker for disease monitoring and therapeutic response. Therefore, further exploration into lactylation's multifaceted role is essential for elucidating its diagnostic potential in PH.

This research establishes a lactylation signature model to predict diagnostic profiles, immune infiltration dynamics, and transcriptional networks in PH (Figure 1). By integrating differentially expressed genes (DEGs) from the GSE15197 dataset with Gene Ontology (GO) and Kyoto Encyclopedia of Genes and Genomes (KEGG) pathway analyses, key molecular pathways involved in PH pathogenesis were identified. Weighted gene co-expression network analyses (WGCNA) further revealed critical lactylation-associated modules, underscoring their functional relevance in PH. Using machine learning algorithms – specifically random forest (RF) and support vector machine (SVM) – we prioritized three hub genes that exhibited both strong predictive performance and significant associations with immune cell infiltration. This multi-modal strategy highlights the potential of lactylation in PH pathogenesis and offers a foundation for novel diagnostic and therapeutic approaches.

## 2. Materials and methods

### 2.1. Data collection and processing

Two datasets (GSE15197 and GSE117261) were obtained from the Gene Expression Omnibus repository[16] (https://www.ncbi.nlm.nih.gov/geo/), as summarized in Table 1. The GSE15197 dataset comprises 18 samples from patients with PH and 13 samples from matched control subjects without PH. In parallel, GSE117261 includes 58 samples from PH patients and 25 samples from demographically matched non-PH control subjects. Differential gene expression analysis between PH patients and controls was conducted using the "limma" package.[17] Visualizations were generated using the "ggplot2"[18] and "heatmap"[19] packages.

### 2.2. Enrichment analyses

DEGs were selected using thresholds of $|\log_2(\text{fold change})| > 0.2$ and adjusted $p<0.05$. To explore the biological mechanisms underlying PH-related DEGs, functional enrichment analyses were performed using

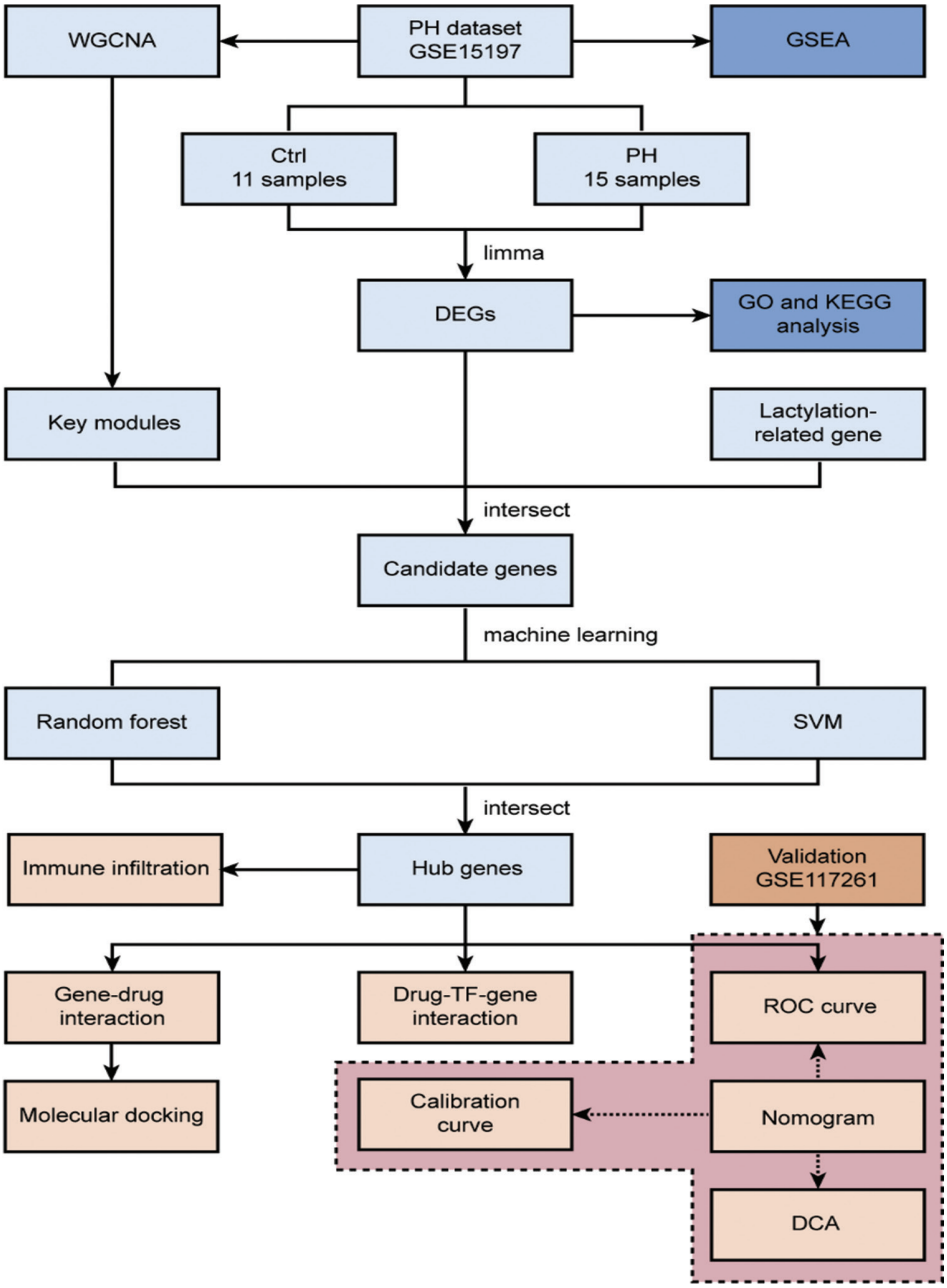


**Figure 1.** Study design overview. This integrated bioinformatics and computational workflow was designed to identify and validate key lactylation-related genes associated with PH, using the GSE15197 dataset. The analyses began with the identification of biologically relevant gene modules significantly correlated with PH (15 samples) compared to controls (Ctrl; 11 samples), using WGCNA. Concurrently, DEGs between the PH and Ctrl groups were determined. GSEA was then performed on the key modules. A curated list of lactylation-related genes was integrated, and the intersection of significant WGCNA modules, DEGs, and lactylation-related genes yielded candidate genes. Machine learning techniques, specifically random forest and SVM, were applied to prioritize the most robust candidate genes, leading to the identification of hub genes. The immune cell infiltration landscape in PH samples was also analyzed. Identified hub genes were validated using an independent dataset (GSE117261). To explore therapeutic potential, gene–drug interaction networks and drug–TF–gene regulatory networks were constructed. The diagnostic power of the hub genes for distinguishing PH was evaluated using ROC curve analyses. Clinical prediction models were also developed, including a nomogram incorporating the hub genes for risk prediction, calibration curves to assess model accuracy, and DCA to evaluate clinical utility. Finally, molecular docking simulations were conducted to investigate potential binding interactions between hub genes and candidate therapeutic compounds, suggesting potential mechanistic pathways and drug targets Abbreviations: PH: Pulmonary hypertension; WGCNA: Weighted Gene Co-expression Network Analyses; GESA: Gene Set Enrichment Analyses; DEGs: differentially expressed genes; SVM: Support vector machine; TF: Transcription factor; ROC: Receiver operating characteristic; DCA: Decision curve analysis.

**Table 1. Characteristics of gene expression datasets analyzed in this study**

| Series | Platform (manufacturer) | Array design | Probe count | Species | Tissue |
|---|---|---|---|---|---|
| GSE15197 | GPL6480 (Agilent Technologies) | Agilent-014850 Whole Human Genome Microarray 4×44K | 41,000+probes | Human | Lung tissue |
| GSE117261 | GPL6244 (Affymetrix) | [HuGene-1_0-st] Affymetrix Human Gene 1.0 ST Array | 28,869 genes | Human | Lung tissue |

the "clusterProfiler"[20] and "org.Hs.eg.db"[21] packages. Terms with adjusted $p<0.05$ were considered significantly enriched. GO/KEGG pathway visualizations results were generated using the "ggplot2"[18] and "GOplot"[22] packages.

### 2.3. WGCNA

To examine gene expression patterns, WGCNA was conducted on the GSE15197 dataset employing the "WGCNA" R package[23] to identify modules significantly associated with PH. The data were preprocessed to remove outliers, followed by the construction of a co-expression matrix using the "WGCNA" package. An optimal soft-thresholding power was determined and applied to transform the matrix into an adjacency matrix. This was then used to compute a topological overlap matrix (TOM), followed by hierarchical clustering with average linkage based on TOM-derived dissimilarity. To evaluate associations between PH and the resulting gene modules, clinically pertinent modules were identified based on gene significance >0.2 and module membership >0.8. Two modules demonstrating the strongest correlation with PH were selected for further analysis.

### 2.4. Diagnostic model development

Candidate genes were identified from the intersection of DEGs, key module genes, and lactylation-associated genes. Two machine learning algorithms – RF and SVM – were then employed to identify hub genes and construct a diagnostic model for PH. The optimal number of variables was determined using the "random forest" R package,[24] which calculated the average error rate for the candidate genes. In addition, an SVM model[25] was constructed using a five-fold cross-validation approach. Hub genes were prioritized based on MeanDecreaseGini scores exceeding a defined threshold in the RF model, combined with features selected by the SVM, to establish the final diagnostic model.

### 2.5. Assessment of the diagnostic model

The diagnostic performance of the model was evaluated using the area under the receiver operating characteristic (ROC) curve (AUC) to assess the capability of hub genes to distinguish PH in the GSE15197 dataset. An AUC value >0.7 was considered indicative of strong diagnostic potential. A nomogram was then constructed using the hub genes with the "rms" package[26] in the GSE117261 dataset. To further evaluate the nomogram's predictive accuracy for lactylation-associated PH, calibration curves and DCA were generated. ROC evaluation was also conducted to quantify the nomogram's diagnostic performance.

### 2.6. Assessment of immune infiltration

Immune infiltration analysis was performed using CIBERSORT[27] to estimate the relative proportions of immune cell types in all samples. The findings were visualized with a bar plot showing immune cell composition across samples. Infiltration scores for 24 immune cell types were calculated using the "GSVA" package through single-sample gene set enrichment analyses (ssGSEA).[28] A box plot was generated to compare the immune cell types between the PH and control groups. Spearman's rank correlation was employed to assess associations between each hub gene and the 24 immune cell types. The "corrplot" R package[29] was used to generate correlation matrices visualizing: (i) interactions among infiltrating immune cells, and (ii) associations between hub gene signatures and immune infiltration patterns.

### 2.7. Identification of TFs related to hub genes

An interaction network between TFs and hub genes was constructed to identify regulatory mechanisms. TFs are specialized proteins that modulate gene expression by activating or suppressing target genes. To ascertain TFs associated with the identified hub genes, we used the "enrichR" R package[30] (https://github.com/compbiomed). The analysis involved intersecting a comprehensive list of human TFs, DEGs, and the predicted TFs. Key TFs were visualized using the Sankeymatic platform (https://www.sankeymatic.com/), providing a graphical representation of their interactions with the hub genes.

### 2.8. Development of a gene–drug interaction network

To explore potential drug candidates targeting PH-related hub genes, we queried the DSigDB database through Enrichr,[30] using the "enrichR" R package (https://github.com/compbiomed). The top 10 drugs, ranked by combined scores, were identified as potential therapeutic options. The relationship between the hub genes and these candidate drugs was visualized using Sankeymatic (https://www.sankeymatic.com/), offering insights into potential drug–target interactions.

### 2.9. Molecular docking studies

Protein structures corresponding to the hub genes were retrieved from the UniProt database (https://www.uniprot.org/) and converted into Protein Data Bank (PDB) format after preprocessing. Candidate drug structures were obtained from PubChem (https://pubchem.ncbi.nlm.nih.gov/) and converted to Protein Data Bank, Partial Charge (Q), and Atom Type (T) (PDBQT) format using OpenBabel. Molecular docking was performed using AutoDock Vina.[31] Binding affinities were interpreted as follows: < −7 kcal/mol indicated strong binding; −4 to −7 kcal/mol suggested weak binding; and > −4 kcal/mol indicated no significant interaction.

### 2.10. Statistical analysis

Statistical analyses were performed using R version 4.4.1 (R Foundation for Statistical Computing, Austria). ROC curve evaluation was employed to assess the diagnostic potential of the hub genes in distinguishing between the PH and control groups. A two-tailed $p<0.05$ was considered statistically significant, unless otherwise stated.

## 3. Results

### 3.1. Identification of DEGs

To identify potential biomarkers associated with PH, we analyzed the GSE15197 dataset, which revealed a total of 3,435 DEGs, including 1,504 upregulated and 1,931 downregulated genes (Figure 2A). The top 50 DEGs, selected based on an adjusted $p<0.05$, are shown in a heatmap (Figure 2B).

### 3.2. Functional enrichment analyses

To elucidate the functions and underlying mechanisms of the DEGs, we performed GO and KEGG enrichment analyses. GO analysis demonstrated that the DEGs were enriched in biological processes such as cellular transport, protein catabolism, DNA repair, and signal transduction, which are essential for maintaining cellular homeostasis (Figure 3A). The GO biological process category revealed significant enrichment of PH-related DEGs in the proteasome-mediated ubiquitin-dependent protein catabolic process, viral process, nucleocytoplasmic transport, nuclear transport, and Golgi vesicle transport (Figure 3B). In the cellular component category, DEGs were primarily associated with the mitochondrial matrix, cell–substrate junction, focal adhesion, nuclear speck, and midbody (Figure 3B). Molecular function analysis indicated enrichment in cadherin binding, GTPase activity, ubiquitin-like protein binding, ribosome binding, and ubiquitin binding (Figure 3B). KEGG pathway analysis further showed significant enrichment in biological cascades implicated in PH, including protein processing in the endoplasmic reticulum, epidermal growth factor receptor (EGFR) tyrosine kinase inhibitor resistance, beta-alanine metabolism, tumor necrosis factor (TNF) signaling pathway, and vascular endothelial growth factor (VEGF) signaling pathway (Figure 3C).

### 3.3. WGCNA in PH

To identify PH-associated gene modules, WGCNA was applied to the GSE15197 dataset. The analyses, based on scale independence and average connectivity, successfully identified several modules of interest with significant relevance to the pathophysiology of PH. A soft thresholding power of 11 was selected for the analyses, as illustrated in Figure 4A. Figure 4B shows the clustering of the module eigengenes. Utilizing this thresholding power, we identified a total of seven unique modules. Module clustering patterns are visualized in the dendrogram

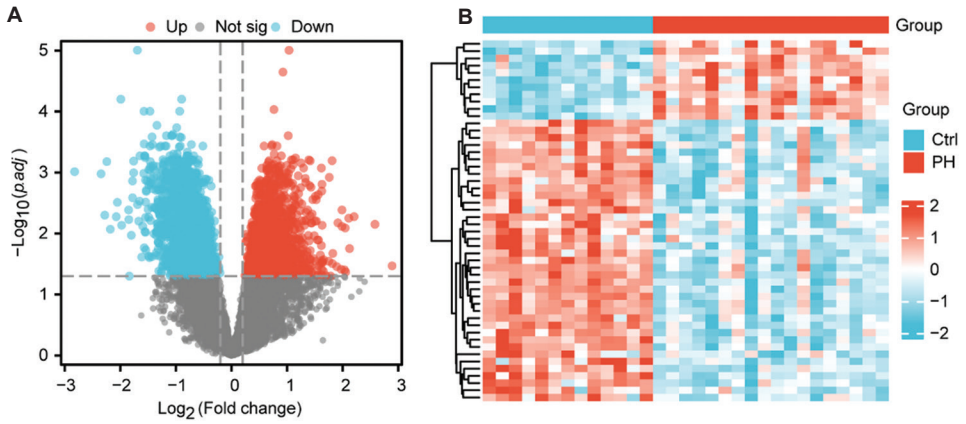


**Figure 2.** Differential expression analysis in the PH dataset. (A) Volcano plot of DEGs in GSE15197, with upregulated (Up) genes in red and downregulated (Down) genes in blue. (B) Heatmap of the top 50 most significantly DEGs in GSE15197.
Abbreviations: adj: Adjusted; ctrl: Control; sig: Significant; PH: Pulmonary hypertension; DEGs: differentially expressed genes.

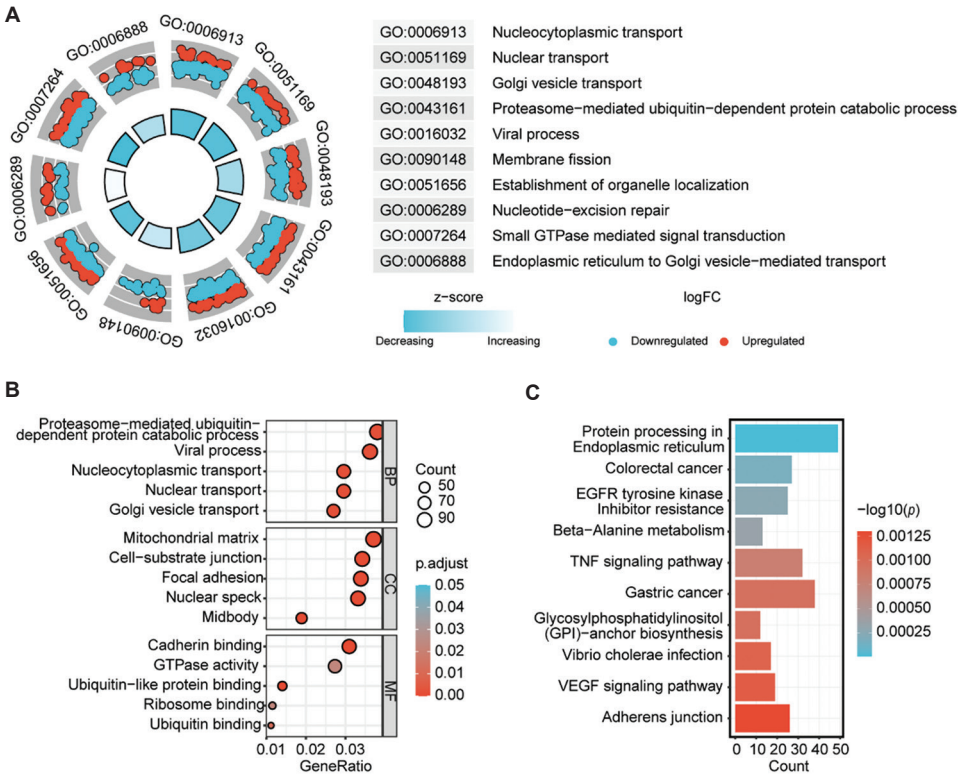


**Figure 3.** Enrichment analyses of differentially expressed genes DEGs. (A) GO Circle plot highlighting significant GO terms. (B) Bubble plots showing the results of GO analyses, including biological processes, molecular functions, and cellular components related to the DEGs. (C) A bar plot illustrating the outcomes of the KEGG pathway analyses related to the DEGs.
Abbreviations: EGFR: Epidermal growth factor receptor; TNF: Tumor necrosis factor; VEGF: Vascular endothelial growth factor; DEGs: Differentially expressed genes; GO: Gene Ontology; KEGG: Kyoto Encyclopedia of Genes and Genomes.

(Figure 4C). We next evaluated the correlations between modules and PH (Figure 4D), revealing: (i) magenta module (289 genes): strongest positive association ($r$ = 0.63, $p$=1e−04); and (ii) greenyellow module (889 genes): most significant negative correlation ($r$ = −0.69, $p$=2e−05). These critical modules were prioritized for subsequent analyses. Inter-modular eigengene relationships showed significant interactions (Figure 4B and E). Strong concordance was observed between module membership and gene significance: magenta module: $r$ = 0.6, $p$=1.8e−86 (Figure 4F); greenyellow module: $r$ = 0.52, $p$=1e−200 (Figure 4G). Ultimately, 1,178 PH-correlated genes were identified.

### 3.4. Identification of diagnostically relevant hub genes via machine learning

We next applied machine learning to identify diagnostically relevant hub genes. By intersecting WGCNA module genes, DEGs, and lactylation-associated genes, we identified 33 PH-related candidate genes (Figure 5A). Figure 5B illustrates the convergence of Out-Of-Bag (OOB) error, PH error, and Ctrl error as the number of decision trees increases, with the errors stabilizing around 30 to 90 trees. These were used to construct a PH diagnostic model. The RF algorithm assessed feature importance among the 33 candidates, selecting five genes with Importance >1 (Figure 5C). Concurrently, SVM analysis identified five genes demonstrating minimal five-fold cross-validation error and maximal accuracy (Figure 5D and E). Intersection of RF-selected and SVM-selected genes revealed three consensus hub genes: Aryl hydrocarbon receptor (*AHR*), polyribonucleotide nucleotidyltransferase 1 (*PNPT1*), and RAS p21 protein activator 1 (*RASA1*) (Figure 5F). These biomarkers show significant diagnostic potential for PH.

### 3.5. Diagnostic validation of three hub genes and nomogram performance

We validated the three hub genes and assessed the nomogram's diagnostic utility. ROC analysis quantified the AUC values for individual hub genes and the combined model, evaluating their diagnostic sensitivity and specificity for PH. All three hub genes demonstrated exceptional diagnostic capacity, with AUC >0.9 (Figure 6A). To establish clinical applicability, we constructed a nomogram using the

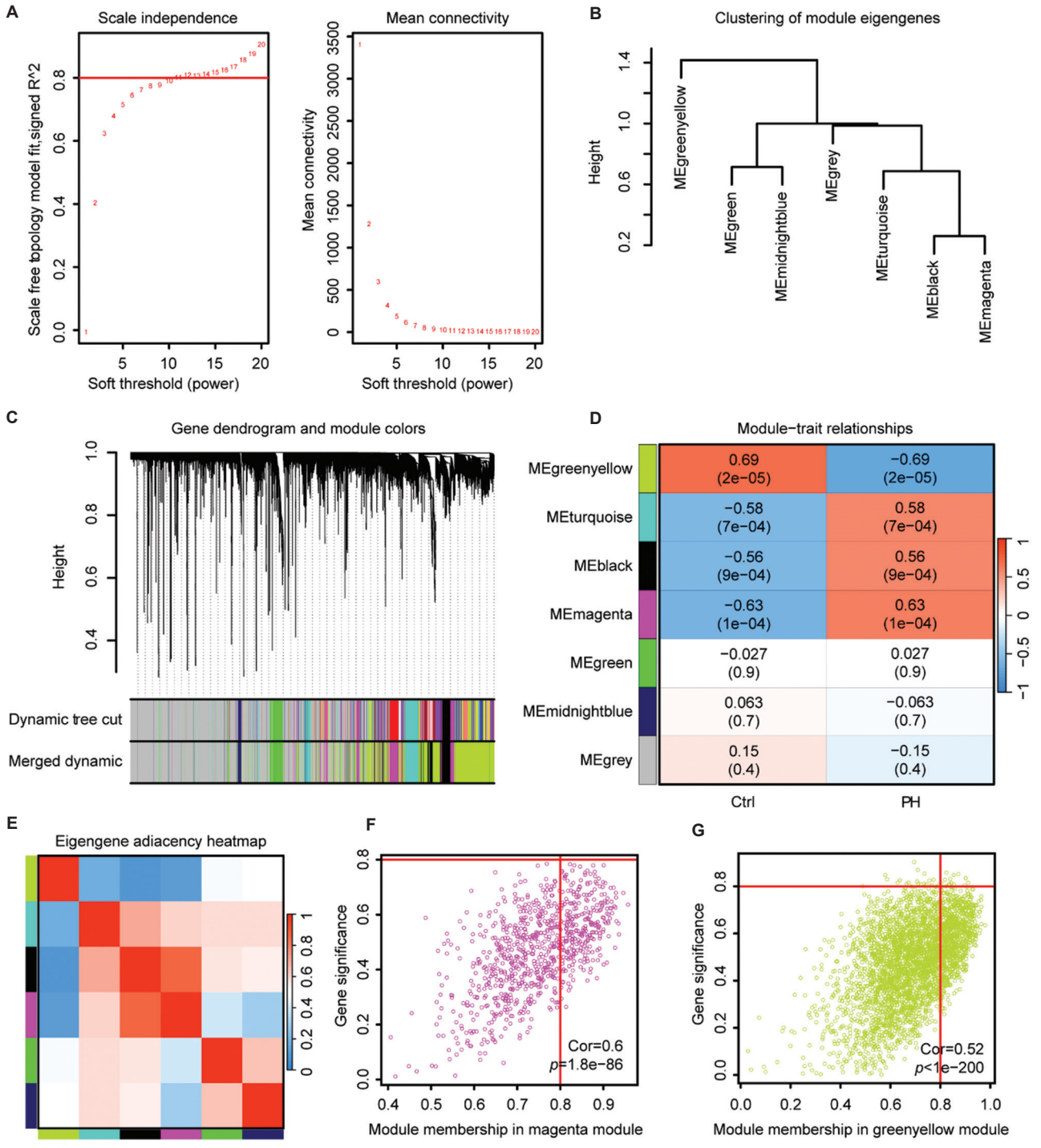


**Figure 4.** Identification of key modules within the GSE15197 dataset through weighted gene co-expression network analyses. (A) Determination of the optimal soft threshold, with β = 11 deemed most suitable. (B) Cluster dendrogram showcasing module eigengenes. (C) Distinct modules illustrated in various colors, obtained by clustering strongly correlated genes; the greenyellow module represents the largest proportion. (D) Eigengene–pulmonary hypertension relationship matrix displaying correlation (Cor) coefficients and *p*-values. (E) Module interaction network showing cross-modular connections. (F) Magenta module: gene significance versus membership correlation. (G) Greenyellow module: constituent gene significance versus module membership association.

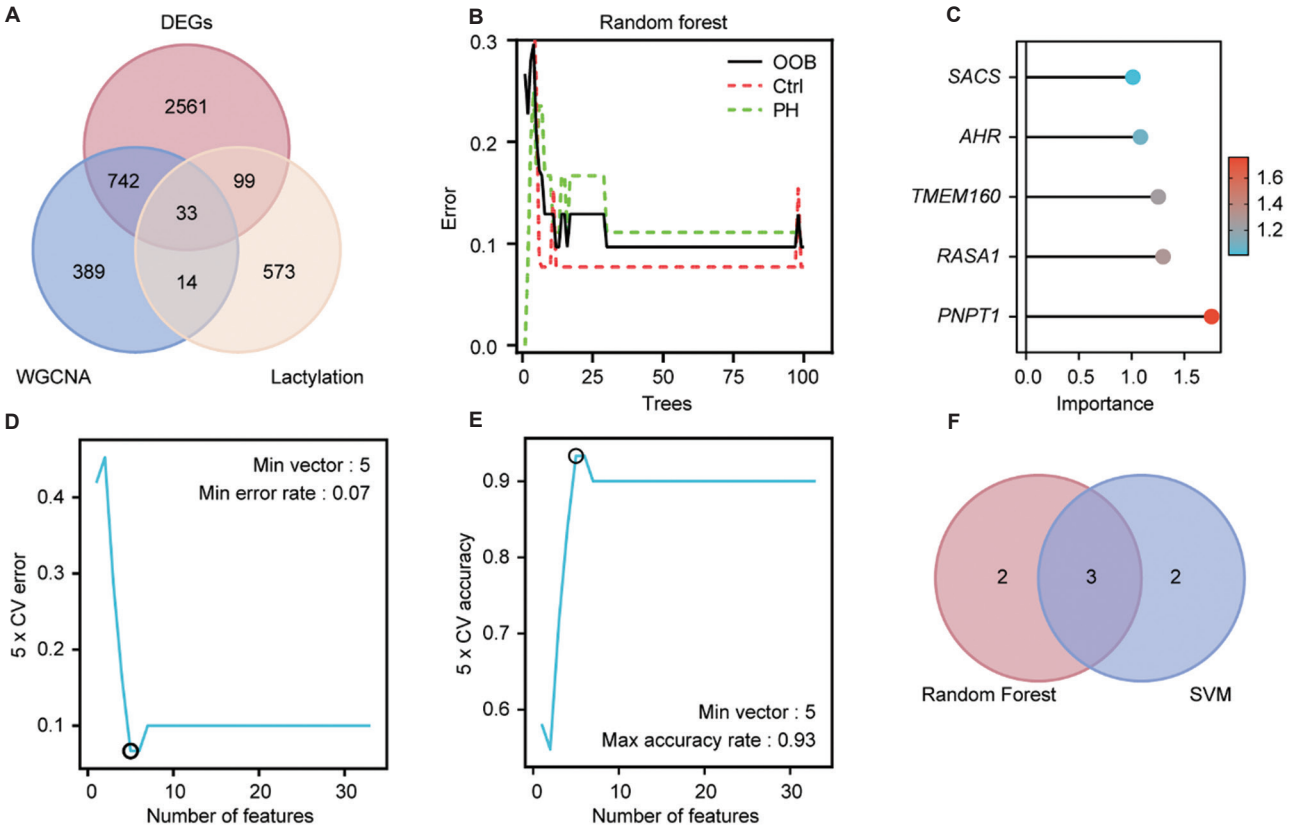


**Figure 5.** Discovery of hub genes linked to lactylation-related PH utilizing machine learning methodologies. (A) Venn diagram showing the overlap of 33 consensus genes among DEGs, lactylation-associated genes, and WGCNA-identified key modules. (B) Error rate variation relative to the number of decision trees. (C) RF feature importance ranking by Gini coefficient. (D) SVM-identified the top 10 low-error genes. (E) SVM-selected top 10 high-accuracy genes. (F) Intersection of RF-/SVM-selected genes: lactylation-related PH hub genes. Abbreviations: Ctrl: Control; OOB: Out-of-bag; Max: Maximum; Min: Minimum; RF: Random forest; PH: Pulmonary hypertension; DEGs: Differentially expressed genes; SVM: Support vector machine; WGCNA: Weighted gene co-expression network analyses.

GSE117261 dataset (Figure 6B). Calibration curves showed strong agreement between nomogram predictions and ideal outcomes (Figure 6C). DCA confirmed the model's clinical value for PH risk assessment (Figure 6D). The nomogram achieved an AUC of 0.820 in validation testing (Figure 6E), supporting its utility as a diagnostic instrument.

### 3.6. Investigation of immune cell infiltration and the relationship of key genes with immune cells in PH

We investigated immune cell infiltration and the correlation of hub genes with immune cells in PH. Functional and pathway analyses associated with PH revealed a significant link to inflammatory and immune pathways. Using the CIBERSORT and ssGSEA algorithms, we profiled immune cell compositions, explored immunoregulatory mechanisms, and evaluated hub gene–immune cell infiltration relationships in PH. Figure 7A shows the distribution patterns of 22 immune cell subsets across samples. Significant abundance differences emerged between the PH and control groups for seven immune cell types (Figure 7B). PH specimens exhibited elevated infiltration of cluster of differentiation (CD)$8^+$ T lymphocytes, immature dendritic cells, and natural killer (NK) cells. Conversely, reduced levels were observed for eosinophils, mast cells, central memory T cells (Tcm), and T helper (Th) cells. Correlation analysis of 24 immune cell types (Figure 7C) revealed the following: (i) strong positive association between Tcm and Th cells ($r = 0.779$, $p<0.05$); and (ii) significant negative correlation between Th and NK cells ($r = -0.647$, $p<0.05$). Furthermore, we examined the relationships between the three hub genes (*AHR*, *PNPT1*, and *RASA1*) and immune cell infiltration. Figure 7D demonstrates significant correlations with Th cells, Tcm, eosinophils, NK cells, and γδ T cells, indicating broad immunomodulatory roles in PH pathogenesis.

### 3.7. Interactions between TFs and hub genes

To explore interactions between TFs and hub genes, we identified 125 TFs associated with hub genes using the Enrichr tool. An overlap of DEGs, all identified human

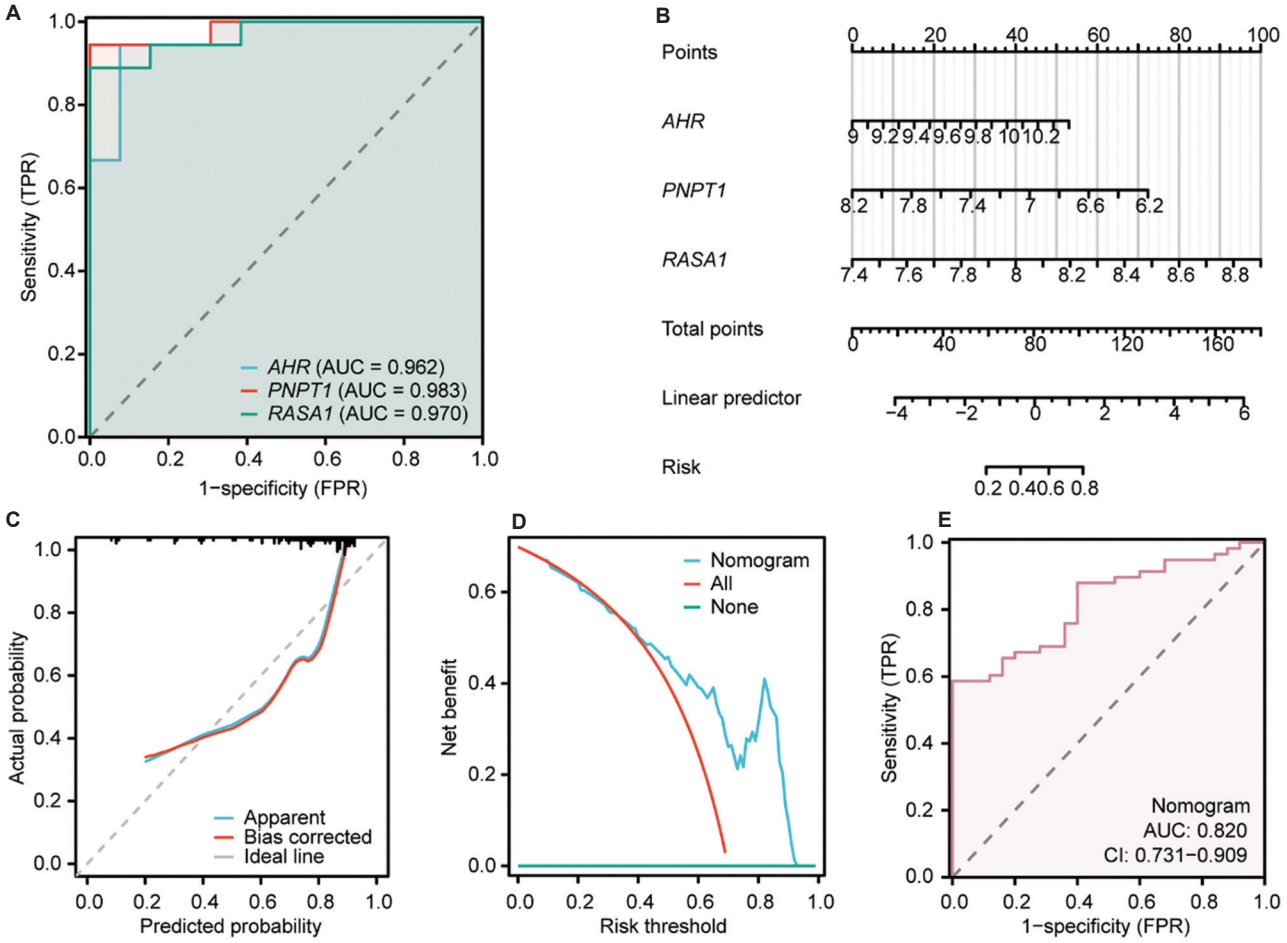


**Figure 6.** Diagnostic performance evaluation of hub genes and nomogram. (A) Receiver operating characteristic (ROC) curves depicting the diagnostic performance of individual hub genes (*AHR*, *PNPT1*, *RASA1*) in GSE15197. (B) Pulmonary hypertension risk assessment nomogram integrating hub genes (GSE117261 cohort). (C) Nomogram calibration curve. (D) Decision curve analysis of the model. (E) Receiver operating characteristic curve validating the nomogram's predictive capacity.
Abbreviations: AUC: Area under the curve; CI: Confidence interval; FPR: False positive rate; TPR: True positive rate.

TFs, and predicted TFs associated with hub genes resulted in the identification of 10 prospective TFs that may modulate hub gene activity (Figure 8A). Furthermore, we constructed a TF–hub gene interaction network (Figure 8B), revealing that *AHR* is regulated by three TFs, *PNPT1* by seven TFs, and *RASA1* by four TFs. Notably, friend leukemia integration 1 (FLI1) TF exhibited the highest cumulative binding score, highlighting its critical role in regulating *AHR* and *PNPT1* expression.

### 3.8. Interactions between hub genes and drugs, along with molecular docking

Regarding the gene–drug interactions, we selected 10 potential drug candidates: estradiol, benzo[a]pyrene, 5-amino-2-methylphenol, phosalone, profenofos, propyl gallate, cyprodinil, isocarbophos, 2,4-dinitrophenol, and iprodione, to establish a hub gene–drug interaction network (Figure 9A). To validate the network findings, molecular docking was performed to assess interactions between candidate drugs and their target hub genes. Summarized drug–gene data are presented in Tables 2 and 3. Figure 9B displays binding affinity values (kcal/mol) for hub gene–drug complexes. The docking analyses showed that the free binding energies ranged from –4.8 to –8.9 kcal/mol, suggesting all drugs formed interactions with the hub genes. Notably, estradiol and benzo[a]pyrene demonstrated strong binding affinities with all three hub genes. The interaction between *AHR* and benzo[a]pyrene yielded the highest binding energy at –8.9 kcal/mol. This interaction was visualized using PyMoL (Figure 9C). The observed binding affinities were primarily attributed to hydrophobic interactions involving residues such as LEU-122C, ASN-123C, ILE-168D, ALA-172D, ILE-268C, PRO-271C, THR-309D, ILE-340D, and THR-378B of *ACADM*, as well as

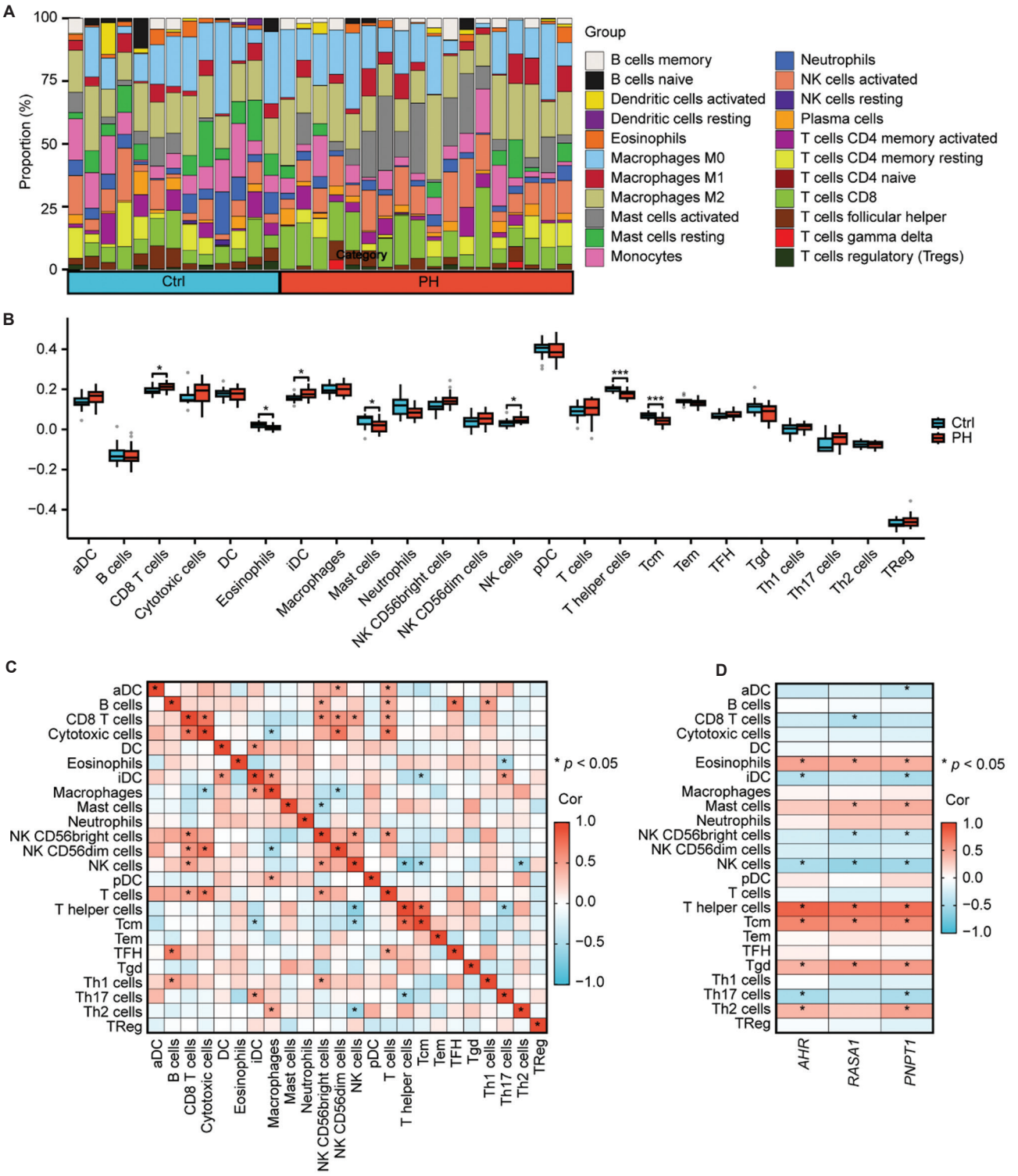


**Figure 7.** Immune microenvironment profiling in PH. (A) Comparative immune cell composition between the PH and control (Ctrl) cohorts (stacked bar chart). (B) Box plot comparing 24 distinct types of immune cells between PH and Ctrl groups, with significance levels indicated as *$p$<0.05, **$p$<0.01, and ***$p$<0.001. (C) Heatmap depicting correlations among infiltration levels of the 24 immune cell types, with significance at *$p$<0.05. (D) Correlation matrix showing associations between infiltrating immune cells and the three hub genes, with significance indicated at *$p$<0.05. Abbreviations: PH: Pulmonary hypertension; aDC: Activated dendritic cells; CD: Cluster of differentiation; cor: Correlation; DC: Dendritic cells; iDC: Immature dendritic cells; NK: Natural killer; pDC: Plasmacytoid dendritic cells; Tcm: Central memory T cells; Tem: Effector memory T cells; TFH: T follicular helper cells; Tgd: γδ T cells; Th: T helper cells; TReg: Regulatory T cells.

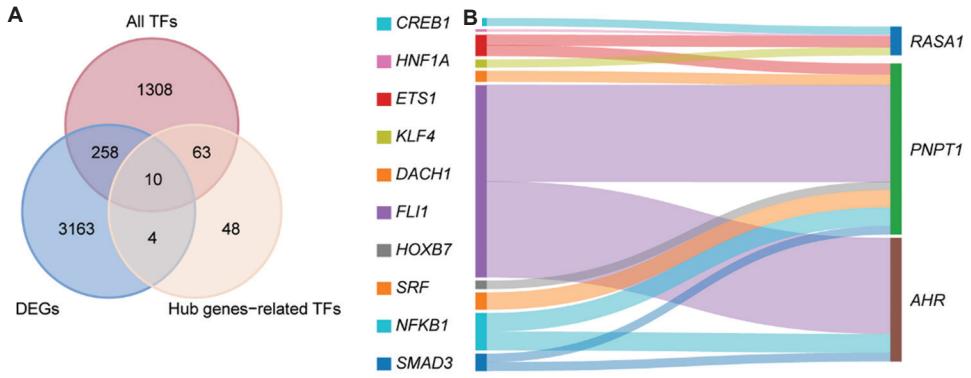


**Figure 8.** Regulatory network of TFs and hub genes. (A) Venn diagram showing overlap among DEGs, predicted TF of hub genes, and human TFs. (B) Sankey visualization mapping relationships between hub genes and candidate TFs.
Abbreviations: TFs: Transcription factors; DEGs: Differentially expressed genes.

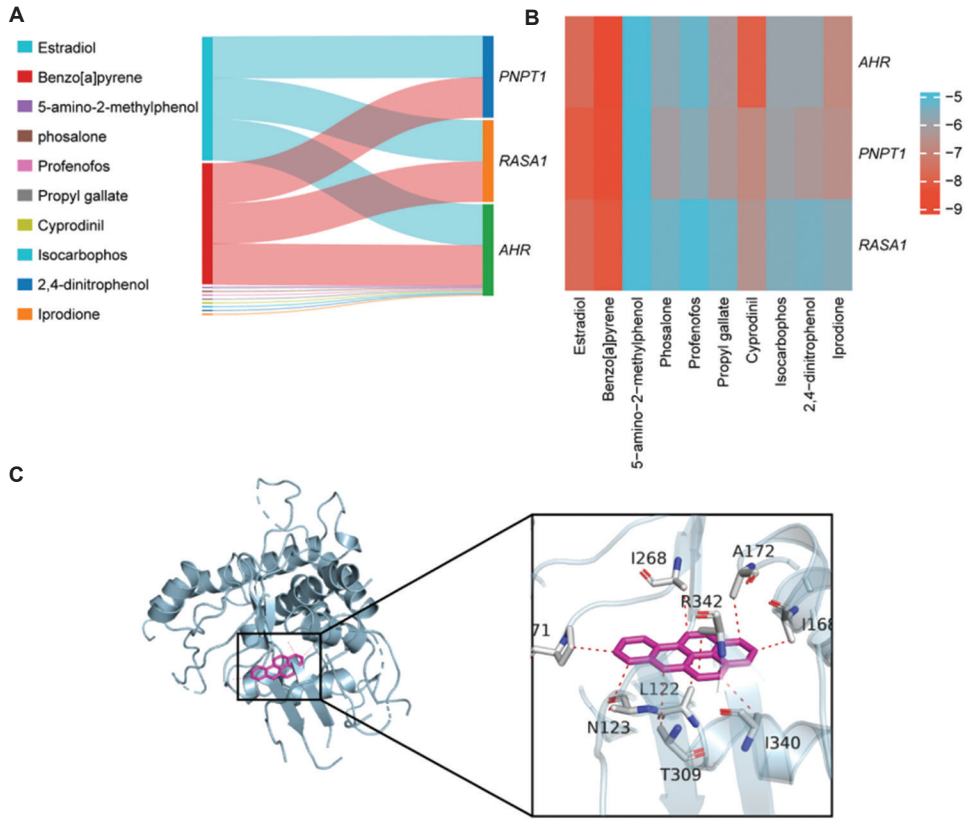


**Figure 9.** Development of the interaction network between drugs and hub genes, along with molecular docking analyses. (A) Sankey diagram illustrating connections between hub genes and candidate drugs. (B) Heatmap displaying binding affinity scores for hub genes against 10 drug candidates from docking studies. (C) Docking configuration of the aryl hydrocarbon receptor–benzo[a]pyrene interaction.

hydrogen bonding with THR-136B, GLU-376B, and ARG-342D residues of *AHR* (Figure 9C). These findings suggest that the selected drugs have therapeutic potential for PH. The application of molecular docking technology provides a valuable approach for evaluating binding interactions between candidate therapeutic agents and hub genes associated with PH. However, it is important to emphasize that further experimental validation is required to confirm the therapeutic efficacy of these candidates.

## 4. Discussion

PH is characterized by increased pulmonary vascular resistance and marked alterations in vascular structure,

**Table 2. Details of drugs selected for molecular docking**

| Drug name | PubChem CID | Molecular weight (Da) |
|---|---|---|
| Estradiol | 5757 | 272.4 g/mol |
| Benzo[a] pyrene | 2336 | 252.3 g/mol |
| 5-amino-2-methylphenol | 17818 | 123.15 g/mol |
| Phosalone | 4793 | 367.8 g/mol |
| Profenofos | 38779 | 373.63 g/mol |
| Propyl gallate | 4947 | 212.2 g/mol |
| Cyprodinil | 86367 | 225.29 g/mol |
| Isocarbophos | 90479 | 289.29 g/mol |
| 2,4-dinitrophenol | 1493 | 184.11 g/mol |
| Iprodione | 37517 | 330.16 g/mol |

**Table 3. A comprehensive overview of the key hub genes selected for molecular docking analyses**

| Gene name | PDB ID |
|---|---|
| *AHR* | 5NJ8 |
| *PNPT1* | 3U1K |
| *RASA1* | 6WAY |

Abbreviations: PDB: Protein Data Bank; *AHR:* Aryl hydrocarbon receptor; *PNPT1*: Polyribonucleotide nucleotidyltransferase 1; *RASA1*: RAS p21 protein activator 1.

leading to right ventricular hypertrophy, heart failure, and an elevated risk of early mortality. Despite notable advancements in treatment modalities, the pursuit of reliable biomarkers for early detection and effective therapeutic interventions remains a substantial challenge.[32,33] Recent investigations have suggested that lactylation plays a significant role in the pathophysiological mechanisms underlying PH. A comprehensive understanding of the molecular mechanisms associated with lactylation in the context of PH could pave the way for the development of innovative diagnostic markers and targeted therapies, ultimately improving patient outcomes. The aim of this research was to formulate a lactylation-associated model for diagnosing and treating PH utilizing a bioinformatics framework. Initially, we carried out differential expression profiling to identify DEGs linked to PH. We then conducted GO and KEGG analyses to investigate the associated biological processes and pathways. Subsequently, we used WGCNA to identify significant gene clusters. These clusters were integrated with DEGs and lactylation-related genes to determine possible candidate genes. Machine learning techniques were applied to narrow down these candidates to three hub genes, which were later incorporated into a diagnostic nomogram. This approach highlights the relationship between lactylation and PH, establishing a foundation for further investigations into immune dysregulation, transcriptional regulation, and potential therapeutic interventions in the treatment of PH.

Mapping the primary signaling pathways contributing to PH is vital for deciphering its pathogenesis and establishing effective therapeutic strategies. In our study, the identification of key signaling pathways, including the TNF and VEGF signaling pathways, enhances our understanding of PH pathophysiology. Recent studies support our conclusion that the TNF signaling pathway plays a crucial role in PH. One study showed that TNF-α enhances the proliferation and migration of vascular smooth muscle cells, contributing significantly to the vascular remodeling associated with chronic thromboembolic PH.[34] In addition, TNF-α-induced pyroptosis, a form of programmed cell death occurring in human pulmonary arterial endothelial cells, has been associated with the progression of PH.[35] Collectively, these findings emphasize the central role of TNF signaling in the pathophysiology of PH. Moreover, the VEGF signaling pathway is intricately involved in PH, with context-dependent effects.[36] Inhibition of this pathway, specifically through deletion of VEGFR2 in endothelial cells, exacerbates pulmonary vascular remodeling and promotes PH progression.[37] Conversely, VEGF overexpression appears to confer protective effects against PH progression.[37] Furthermore, PH is linked to increased pulmonary vascular leakage in both affected individuals and hypoxic murine models, attributed to hyperactivation of the VEGF-A/VEGFR2 Y949 signaling pathway.[38] Notably, elimination of VEGFR2 Y949 signaling through the Y949F mutation prevents pulmonary vascular permeability and inhibits PH, while conditional deletion of *VEGFR2* in endothelial cells accelerates disease progression.[38] Understanding the interplay between these signaling pathways may facilitate the discovery of novel biomarkers and therapeutic targets for PH.

The identification of the hub genes *AHR*, *PNPT1*, and *RASA1* provides a vital foundation for advancing research into PH. The implications of targeting these genes through innovative therapeutic interventions could lead to improved management of this complex disease. Subsequent research efforts should prioritize the validation of these biomarkers and assess the effectiveness of *AHR* inhibition and other novel approaches in clinical settings, ultimately enhancing patient outcomes in PH. Recent studies underscore the critical role of AHR in the pathogenesis of PH. A key study showed that AHR activation is crucial for the development of PH in rats exposed to Sugen 5416 and hypoxia.[39] Notably, the AHR antagonist CH223191 was effective in reversing these effects, indicating that inhibiting *AHR* could represent a novel therapeutic strategy for PH.[39] Furthermore, increased AHR agonistic

activity in the serum of PH patients has been correlated with adverse clinical outcomes, establishing a significant link between AHR and inflammatory responses.[40] Recent findings reveal that a specific AHR ligand, 3'-19 oxo-tabernaelegantine A, can induce selective relaxation of pulmonary arteries, suggesting a potential mechanism involving *AHR* inhibition.[41] Nevertheless, the role of two additional hub genes, *PNPT1* and *RASA1*, in PH remains unvalidated, underscoring a critical area for future investigation. PNPT1 is known to participate in mitochondrial function and lipid metabolism, suggesting a potential role under the hypoxic conditions frequently observed in PH.[42,43] Similarly, RASA1 is implicated in the modulation of Ras signaling pathways, which are essential for cellular proliferation and survival – processes central to the vascular remodeling observed in PH.[44] Together, the hub genes AHR, PNPT1, and RASA1 offer valuable insights into the pathophysiological mechanisms of PH and highlight promising avenues for diagnostics and therapeutic development, warranting further exploration of their functions and clinical significance.

Moreover, analyses of immune cell infiltration in PH revealed marked disparities in the levels of specific cell types, such as Th cells, NK cells, and eosinophils, which are key players in inflammatory responses and tissue healing. Th cells, especially Th17 cells, are especially relevant in PH, as they influence both inflammation and vascular remodeling. Studies indicate that Th17 cells play a crucial role in the progression of chronic hypoxia-induced PH, with depletion of $CD4^+$ T cells or inhibition of Th17 differentiation preventing pulmonary remodeling.[45] In addition, interleukin-6 signaling in $CD4^+$ T cells is pivotal in the development of PH; its disruption leads to symptom improvement in hypoxia-induced PH.[46] NK cells, essential components of the innate immune response, are also implicated in PH. A recent study found that the absence of NK cells in the pulmonary microenvironment of murine models correlates with increased expression of the TF Fra-20, which is linked to systemic sclerosis (SSc) and PH.[47] Another study suggested that NK cell deficiency disrupts the signal transducer and activator of transcription 1–chemokine (C-X-C motif) ligand (CXCL) 9–C-X-C motif chemokine receptor 3 signaling pathway in pulmonary fibrosis-related PH.[48] Notably, reactivating this pathway through NK cell activation may represent a novel therapeutic strategy for managing PH.[48] Eosinophils also play a complex role in the progression of PH. On one hand, they are implicated in the exacerbation of PH, as adiponectin deficiency may worsen the condition by promoting the recruitment of eosinophils into pulmonary tissues, highlighting their significant contribution to the inflammatory processes underlying the pathogenesis of PH.[49] On the other hand, eosinophils may exert protective effects in specific contexts by mitigating perivascular inflammation and preserving the homeostasis of pulmonary arterial smooth muscle cells through the action of 14/17-HDHA.[50] The interactions among T cells, NK cells, and eosinophils, potentially influenced by the hub genes identified in this study, reveal intricate immune dynamics in PH. These insights deepen our understanding of disease mechanisms and provide a direction for future research focused on targeting immune pathways for therapeutic benefit.

In addition, this research identified FLI1 as the most promising TF linked to lactylation in PH, thereby providing insights into the regulatory mechanisms governing this condition. Existing research indicates that FLI1 plays a critical role in PH, especially in the context of SSc. The absence of FLI1 is associated with the upregulation of endothelial adipsin, which has been implicated in the progression of PH in SSc.[51] Furthermore, FLI1 deficiency is linked to elevated levels of CXCL13 in macrophages, which correlate with impaired pulmonary function and a higher prevalence of PH in individuals with SSc.[52]

The exploration of therapeutic agents targeting PH is crucial for improving patient outcomes. Proposed pharmacological agents, including estradiol, benzo[a] pyrene, 5-amino-2-methylphenol, phosalone, profenofos, propyl gallate, cyprodinil, isocarbophos, 2,4-dinitrophenol, and iprodione, represent a diverse range of compounds that may influence lactylation pathways relevant to PH. The effects of estrogens on PH are multifaceted, presenting both beneficial and detrimental outcomes,[53] suggesting that substantial progress is needed before estrogen can be considered a viable treatment option. Similarly, although benzo[a]pyrene is primarily recognized as an environmental toxin, its complex interactions with cellular pathways warrant further investigation. Compounds such as 5-amino-2-methylphenol, known for their industrial applications, may also reveal novel therapeutic opportunities through their engagement with cellular mechanisms pertinent to PH. In addition, the influence of pesticides such as phosalone, profenofos, and isocarbophos on lactylation processes may open new research directions. Furthermore, substances such as cyprodinil and iprodione, commonly used as fungicides, also warrant closer examination regarding their effects on pulmonary vascular remodeling. Propyl gallate, noted for its antioxidant properties, may be pivotal in mitigating oxidative stress linked to PH. The potential involvement of 2,4-dinitrophenol in metabolic regulation[54] further suggests that metabolic modulation could contribute to PH management. Understanding the mechanisms through

which these agents affect lactylation may unveil new therapeutic targets and support the development of more effective treatment methodologies for patients with PH.

This research effectively identifies and validates lactylation biomarkers associated with PH through a rigorous methodological approach that integrates various analytical techniques, thereby establishing a relationship between candidate genes and lactylation-related PH. The incorporation of machine learning algorithms significantly enhanced the identification of key genes and improved diagnostic accuracy, while the analysis of immune infiltration provided essential insights into the immunological characteristics of PH.[55,56] In addition, molecular docking studies investigating drug–gene interactions have strengthened the translational relevance of our findings, contributing meaningfully to PH research. Nonetheless, several limitations must be acknowledged. First, the reliance on a single dataset (GSE15197) may constrain the generalizability of our results. This limitation arises from biological variability across distinct patient populations and clinical settings, which may influence the expression of lactylation-associated genes. Second, although machine learning techniques were employed to identify central genes, the relatively small sample size introduces the risk of overfitting. Furthermore, while molecular docking offered valuable perspectives into drug–gene interactions, further *in vitro* and *in vivo* studies are required to confirm the therapeutic efficacy and safety profile of the identified candidate drugs. Addressing these limitations in future studies is vital for strengthening the reliability and clinical relevance of our findings.

## 5. Conclusion

Our investigation successfully established a diagnostic nomogram related to lactylation for PH, underscoring the potential of lactylation-associated hub genes as novel biomarkers and therapeutic targets. The identification of three hub genes, *AHR*, *PNPT1*, and *RASA1*, is particularly noteworthy, as it underscores the complex interplay between lactylation processes and the pathophysiological mechanisms of PH, especially those involving immune system dysfunction. The nomogram developed in this study exhibited strong diagnostic capabilities, validated in an external cohort, suggesting its potential clinical utility for the rapid detection of PH. Furthermore, our analysis of immune cell infiltration, along with predictions of potential therapeutic compounds, lays the groundwork for future investigations aimed at elucidating the therapeutic relevance of lactylation-related pathways. Collectively, these findings not only enhance our understanding of lactylation's role in PH but also provide a foundation for the development of future therapeutic strategies targeting lactylation-associated genes.

## Acknowledgments

None.

## Funding

The study was supported by the Natural Science Foundation of Shenzhen Municipality (Grant ID: JCYJ20230807114505010).

## Conflict of interest

The authors declare that they have no competing interests.

## Author contributions

*Conceptualization:* Qian Lei
*Formal analysis:* Tao Yi, Junsheng Sun
*Funding acquisition:* Tao Yi
*Investigation:* Tao Yi, Cuiwen Deng
*Methodology:* Qian Lei, Tao Yi
*Writing–original draft:* Tao Yi, Cuiwen Deng
*Writing–review & editing:* Qian Lei

## Ethics approval and consent to participate

Not applicable.

## Consent for publication

Not applicable.

## Availability of data

The original contributions presented in this research are included in the article and its supplementary materials. Further inquiries can be directed to the corresponding author.

## References

1. Jasemi SV, Khazaei H, Aneva IY, Farzaei MH, Echeverria J. Medicinal plants and phytochemicals for the treatment of pulmonary hypertension. *Front Pharmacol*. 2020;11:145.

   doi: 10.3389/fphar.2020.00145

2. Wang XJ, Xu XQ, Sun K, *et al*. Association of rare PTGIS variants with susceptibility and pulmonary vascular response in patients with idiopathic pulmonary arterial hypertension. *JAMA Cardiol*. 2020;5(6):677-684.

   doi: 10.1001/jamacardio.2020.0479

3. Swift AJ, Dwivedi K, Johns C, *et al*. Diagnostic accuracy of CT pulmonary angiography in suspected pulmonary hypertension. *Eur Radiol*. 2020;30(9):4918-4929.

   doi: 10.1007/s00330-020-06846-1

4. Slegg OG, Willis JA, Wilkinson F, *et al*. IMproving PULmonary hypertension screening by echocardiography: IMPULSE. *Echo Res Pract*. 2022;9(1):9.

doi: 10.1186/s44156-022-00010-9

5. Oliveira AC, Richards EM, Raizada MK. Pulmonary hypertension: Pathophysiology beyond the lung. *Pharmacol Res*. 2020;151:104518.

   doi: 10.1016/j.phrs.2019.104518

6. Wu H, Huang H, Zhao Y. Interplay between metabolic reprogramming and post-translational modifications: From glycolysis to lactylation. *Front Immunol*. 2023;14:1211221.

   doi: 10.3389/fimmu.2023.1211221

7. Zhang D, Tang Z, Huang H, *et al*. Metabolic regulation of gene expression by histone lactylation. *Nature*. 2019;574(7779):575-580.

   doi: 10.1038/s41586-019-1678-1

8. Cui H, Xie N, Banerjee S, *et al*. Lung myofibroblasts promote macrophage profibrotic activity through lactate-induced histone lactylation. *Am J Respir Cell Mol Biol*. 2021;64(1):115-125.

   doi: 10.1165/rcmb.2020-0360OC

9. Chen J, Zhang M, Liu Y, *et al*. Histone lactylation driven by mROS-mediated glycolytic shift promotes hypoxic pulmonary hypertension. *J Mol Cell Biol*. 2023;14(12):mjac073.

   doi: 10.1093/jmcb/mjac073

10. Zhao SS, Liu J, Wu QC, Zhou XL. Role of histone lactylation interference RNA $m^6A$ modification and immune microenvironment homeostasis in pulmonary arterial hypertension. *Front Cell Dev Biol*. 2023;11:1268646.

    doi: 10.3389/fcell.2023.1268646

11. Wan N, Wang N, Yu S, *et al*. Cyclic immonium ion of lactyllysine reveals widespread lactylation in the human proteome. *Nat Methods*. 2022;19(7):854-864.

    doi: 10.1038/s41592-022-01523-1

12. Rabinowitz JD, Enerback S. Lactate: The ugly duckling of energy metabolism. *Nat Metab*. 2020;2(7):566-571.

    doi: 10.1038/s42255-020-0243-4

13. Li X, Yang Y, Zhang B, *et al*. Lactate metabolism in human health and disease. *Signal Transduct Target Ther*. 2022;7(1):305.

    doi: 10.1038/s41392-022-01151-3

14. Wu D, Wang S, Wang F, Zhang Q, Zhang Z, Li X. Lactate dehydrogenase A (LDHA)-mediated lactate generation promotes pulmonary vascular remodeling in pulmonary hypertension. *J Transl Med*. 2024;22(1):738.

    doi: 10.1186/s12967-024-05543-7

15. Jiang L, Zhyvylo I, Goncharov D, *et al*. LDHA-lactate promotes smooth muscle remodeling and pulmonary hypertension through lactylation of TOP1 and EMILIN1. 2023;148(Suppl 1):A14485-A14485.

    doi: 10.1161/circ.148.suppl_1.14485

16. Clough E, Barrett T, Wilhite SE, *et al*. NCBI GEO: Archive for gene expression and epigenomics data sets: 23-year update. *Nucleic Acids Res*. 2024;52(D1):D138-D144.

    doi: 10.1093/nar/gkad965

17. Ritchie ME, Phipson B, Wu D, *et al*. Limma powers differential expression analyses for RNA-sequencing and microarray studies. *Nucleic Acids Res*. 2015;43(7):e47.

    doi: 10.1093/nar/gkv007

18. Hadley W. *Ggplot2: Elegrant Graphics for Data Analysis*. Berlin: Springer; 2016.

19. Kolde R. *Pheatmap: Pretty Heatmaps. R Package Version 1.0. 8*; 2015.

20. Yu G, Wang LG, Han Y, He QY. Clusterprofiler: An R package for comparing biological themes among gene clusters. *OMICS*. 2012;16(5):284-287.

    doi: 10.1089/omi.2011.0118

21. Carlson MJ. *Genome Wide Annotation for Human, Primarily Based on Mapping using Entrez Gene Identifiers*. Vol. 3. Boston: Bioconductor Home; 2015.

22. Walter W, Sanchez-Cabo F, Ricote M. GOplot: An R package for visually combining expression data with functional analysis. *Bioinformatics*. 2015;31(17):2912-2914.

    doi: 10.1093/bioinformatics/btv300

23. Langfelder P, Horvath S. WGCNA: An R package for weighted correlation network analysis. *BMC Bioinformatics*. 2008;9:559.

    doi: 10.1186/1471-2105-9-559

24. Breiman L. Random forests. *Mach Learn*. 2001;45(1):5-32.

    doi: 10.1023/A:1010933404324

25. Guyon I, Weston J, Barnhill S, Vapnik V. Gene selection for cancer classification using support vector machines. *Mach Learn*. 2002;46:389-422.

    doi: 10.1023/A:1012487302797

26. Harrell FE. *Regression Modeling Strategies*. Berlin: Springer; 2012. p. 6-2.

27. Newman AM, Liu CL, Green MR, *et al*. Robust enumeration of cell subsets from tissue expression profiles. *Nat Methods*. 2015;12(5):453-457.

    doi: 10.1038/nmeth.3337

28. Hanzelmann S, Castelo R, Guinney J. GSVA: Gene set variation analysis for microarray and RNA-seq data. *BMC Bioinformatics*. 2013;14:7.

    doi: 10.1186/1471-2105-14-7

29. Wei T, Simko V, Levy M, Xie Y, Jin Y, Zemla JJS. Package 'corrplot'. *Statistician*. 2017;56(316):e24.

30. Chen EY, Tan CM, Kou Y, *et al*. Enrichr: Interactive and collaborative HTML5 gene list enrichment analysis tool. *BMC Bioinformatics*. 2013;14:128.

doi: 10.1186/1471-2105-14-128

31. Trott O, Olson AJ. AutoDock Vina: Improving the speed and accuracy of docking with a new scoring function, efficient optimization, and multithreading. *J Comput Chem*. 2010;31(2):455-461.

doi: 10.1002/jcc.21334

32. Singh AV, Romeo A, Scott K, *et al*. Emerging technologies for *in vitro* inhalation toxicology. *Adv Healthc Mater*. 2021;10(18):e2100633.

doi: 10.1002/adhm.202100633

33. Singh AV, Maharjan RS, Kromer C, *et al*. Advances in smoking related *in vitro* inhalation toxicology: A perspective case of challenges and opportunities from progresses in lung-on-chip technologies. *Chem Res Toxicol.* 2021;34(9):1984-2002.

doi: 10.1021/acs.chemrestox.1c00219

34. Wang F, Sun C, Lv X, *et al*. Identification of a novel gene correlated with vascular smooth muscle cells proliferation and migration in chronic thromboembolic pulmonary hypertension. *Front Physiol.* 2021;12:744219.

doi: 10.3389/fphys.2021.744219

35. Wu Y, Pan B, Zhang Z, *et al*. Caspase-4/11-mediated pulmonary artery endothelial cell pyroptosis contributes to pulmonary arterial hypertension. *Hypertension*. 2022;79(3):536-548.

doi: 10.1161/HYPERTENSIONAHA.121.17868

36. Gallardo-Vara E, Ntokou A, Dave JM, Jovin DG, Saddouk FZ, Greif DM. Vascular pathobiology of pulmonary hypertension. *J Heart Lung Transplant*. 2023;42(5):544-552.

doi: 10.1016/j.healun.2022.12.012

37. Winter MP, Sharma S, Altmann J, *et al*. Interruption of vascular endothelial growth factor receptor 2 signaling induces a proliferative pulmonary vasculopathy and pulmonary hypertension. *Basic Res Cardiol*. 2020;115(6):58.

doi: 10.1007/s00395-020-0811-5

38. Zhou W, Liu K, Zeng L, *et al*. Targeting VEGF-A/VEGFR2 Y949 signaling-mediated vascular permeability alleviates hypoxic pulmonary hypertension. *Circulation.* 2022;146(24):1855-1881.

doi: 10.1161/CIRCULATIONAHA.122.061900

39. Dean A, Gregorc T, Docherty CK, *et al*. Role of the aryl hydrocarbon receptor in sugen 5416-induced experimental pulmonary hypertension. *Am J Respir Cell Mol Biol*. 2018;58(3):320-330.

doi: 10.1165/rcmb.2017-0260OC

40. Masaki T, Okazawa M, Asano R, *et al*. Aryl hydrocarbon receptor is essential for the pathogenesis of pulmonary arterial hypertension. *Proc Natl Acad Sci U S A*. 2021;118(11):e2023899118.

doi: 10.1073/pnas.2023899118

41. Long P, Li Y, Wen Q, *et al*. 3'-oxo-tabernaelegantine A (OTNA) selectively relaxes pulmonary arteries by inhibiting AhR. *Phytomedicine.* 2021;92:153751.

doi: 10.1016/j.phymed.2021.153751

42. Hsu CG, Li W, Sowden M, Chavez CL, Berk BC. Pnpt1 mediates NLRP3 inflammasome activation by MAVS and metabolic reprogramming in macrophages. *Cell Mol Immunol*. 2023;20(2):131-142.

doi: 10.1038/s41423-022-00962-2

43. Guan C, Zou X, Yang C, *et al*. Polyribonucleotide nucleotidyltransferase 1 participates in metabolic-associated fatty liver disease pathogenesis by affecting lipid metabolism and mitochondrial homeostasis. *Mol Metab*. 2024;89:102022.

doi: 10.1016/j.molmet.2024.102022

44. Zhang Y, Li Y, Wang Q, *et al*. Role of RASA1 in cancer: A review and update (review). *Oncol Rep.* 2020;44(6):2386-2396.

doi: 10.3892/or.2020.7807

45. Maston LD, Jones DT, Giermakowska W, *et al*. Central role of T helper 17 cells in chronic hypoxia-induced pulmonary hypertension. *Am J Physiol Lung Cell Mol Physiol.* 2017;312(5):L609-L624.

doi: 10.1152/ajplung.00531.2016

46. Ishibashi T, Inagaki T, Okazawa M, *et al*. IL-6/gp130 signaling in $CD4^+$ T cells drives the pathogenesis of pulmonary hypertension. *Proc Natl Acad Sci U S A*. 2024;121(16):e2315123121.

doi: 10.1073/pnas.2315123121

47. Schnoegl D, Hochgerner M, Gotthardt D, Marsh LM. Fra-2 is a dominant negative regulator of natural killer cell development. *Front Immunol.* 2022;13:909270.

doi: 10.3389/fimmu.2022.909270

48. Jandl K, Marsh LM, Mutgan AC, *et al*. Impairment of the NKT-STAT1-CXCL9 axis contributes to vessel fibrosis in pulmonary hypertension caused by lung fibrosis. *Am J Respir Crit Care Med*. 2022;206(8):981-998.

doi: 10.1164/rccm.202201-0142OC

49. Weng M, Baron DM, Bloch KD, Luster AD, Lee JJ, Medoff BD. Eosinophils are necessary for pulmonary arterial remodeling in a mouse model of eosinophilic inflammation-induced pulmonary hypertension. *Am J Physiol Lung Cell Mol Physiol.* 2011;301(6):L927-L936.

doi: 10.1152/ajplung.00049.2011

50. Shu T, Zhang J, Zhou Y, *et al*. Eosinophils protect against

pulmonary hypertension through 14-HDHA and 17-HDHA. *Eur Respir J.* 2023;61(3):2200582.

doi: 10.1183/13993003.00582-2022

51. Miyagawa T, Taniguchi T, Saigusa R, *et al*. Fli1 deficiency induces endothelial adipsin expression, contributing to the onset of pulmonary arterial hypertension in systemic sclerosis. *Rheumatology (Oxford).* 2020;59(8):2005-2015.

doi: 10.1093/rheumatology/kez517

52. Taniguchi T, Miyagawa T, Toyama S, *et al*. CXCL13 produced by macrophages due to Fli1 deficiency may contribute to the development of tissue fibrosis, vasculopathy and immune activation in systemic sclerosis. *Exp Dermatol.* 2018;27(9):1030-1037.

doi: 10.1111/exd.13724

53. Tofovic SP, Jackson EK. Estradiol metabolism: Crossroads in pulmonary arterial hypertension. *Int J Mol Sci*. 2019;21(1):116.

doi: 10.3390/ijms21010116

54. Geisler JG. 2,4 dinitrophenol as medicine. *Cells.* 2019;8(3):280.

doi: 10.3390/cells8030280

55. Chandrasekar V, Mohammad S, Aboumarzouk O, Singh AV, Dakua SP. Quantitative prediction of toxicological points of departure using two-stage machine learning models: A new approach methodology (NAM) for chemical risk assessment. *J Hazard Mater*. 2025;487:137071.

doi: 10.1016/j.jhazmat.2024.137071

56. Singh AV, Bhardwaj P, Laux P, *et al*. AI and ML-based risk assessment of chemicals: Predicting carcinogenic risk from chemical-induced genomic instability. *Front Toxicol.* 2024;6:1461587.

doi: 10.3389/ftox.2024.1461587